STM JOURNALS

International Journal of
Cell Biology and Cellular Functions

Volume 1, Issue 1, 2023
January—June
DOI (Journal): 10.37591/IJCBCF

https://journals.stmjournals.com/ijcbcf

Research IJCBCF

Molecular Docking and Pharmacokinetic Profiling of the Phytocompounds of Jatropha curcas as Antagonist for Salmonella typhi

Nayan M.*

Abstract

Background: Typhoid is an infection caused by the Gram-negative bacterium, Salmonella enterica serovar typhi. The study assessed the potential use of Jatropha curcas as a typhoid fever therapy alternative to traditional medications. The ability to uncover novel drug indications for currently available medications using in silico methods has increased thanks to the wealth of pharmacological and biological knowledge that is available. Objective: In this study, we assessed the potential inhibitory effects of phytocompounds from Jatropha curcas against five proteins of Salmonella typhi. Methods: Molecular docking was implemented to evaluate the efficacy of 93 phytocompounds from Jatropha curcas against the target proteins of Salmonella typhi. (Beta-lactamase, DNA Gyrase B, Lactate dehydrogenase, L-lactate dehydrogenase and Retinal dehydrogenase). PyRx, a Virtual Screening software was utilized for molecular docking which allowed the inspection of three-dimensional protein structures and the identification of potential binding sites. ADMET Lab 2.0 was used to evaluate the drug-likeness properties of the phytoconstituents. Results: On analysing the molecular docking results, 4-(P-Methoxyphenyl)-2-(4-phenyl-2-pyridyl)-6-(2-pyridyl)-pyridine, 2-Quinazolinamine, 3,4-dihydro-N,3-diphenyl-4-(phenylimino)-, alpha-Amyrin and Isovitexin exhibited the best binding affinity towards the five target proteins of Salmonella typhi. Conclusion: This study demonstrated that Jatropha curcas is a reliable source of potential phytotherapy for treating Typhoid.

Keywords: Typhoid, Molecular docking, Phytocompounds, Beta-lactamase, DNA Gyrase B, Lactate dehydrogenase, L-lactate dehydrogenase and Retinal dehydrogenase, ADMET, 4-(P-Methoxyphenyl)-2-(4-phenyl-2-pyridyl)-6-(2-pyridyl)-pyridine, 2-Quinazolinamine, 3,4-dihydro-N,3-diphenyl-4-(phenylimino)-, alpha-Amyrin and Isovitexin, Binding affinity.

INTRODUCTION

Typhoid or enteric fever is a bacterial infection that can cause vomiting, diarrhoea, and a high temperature. It is caused by *Salmonella typhi*, a member of the Enterobacteriaceae family. Despite extensive study and public health initiatives, it is still endemic among populations with inadequate access to safe drinking water and sanitation. The bacterium is known to be spread by the 'four Fs' (fingers, flies, fomites, and faeces). Salmonella is more ubiquitous in places where there is social unrest, overcrowding, and inadequate sanitation and is spread through the faecal-oral route through contaminated water, food, and fomites of infected individuals. Humans are its sole host, meaning they can only spread from one sick person to another. Poultry, eggs, and very seldom turtles are the main sources of Salmonella. The normal gut flora is defensive against the infection but is

***Author for Correspondence**
Nayan M.
E-mail: nayanmr19@gmail.com

Student, Department of Biotechnology, MS Ramaiah College of Arts Science & Commerce, 7th Main Rd, MSRIT, M S R Nagar, Mathikere, Bengaluru, Karnataka, India

Received Date: March 02, 2023
Accepted Date: March 31, 2023
Published Date: May 05, 2023

Citation: Nayan M. Molecular Docking and Pharmacokinetic Profiling of the Phytocompounds of Jatropha curcas as Antagonist for Salmonella typhi. International Journal of Cell Biology and Cellular Functions. 2023; 1(1): 67–81p.

© JournalsPub 2023. All Rights Reserved

destroyed upon using antibiotics like streptomycin which accelerates the invasion. Malnutrition reduces healthy gut flora, making people more vulnerable to this illness [1]. As a result, both poor nutrition and the usage of broad-spectrum antibiotics increase the prevalence of typhoid fever.

In accordance with the Global Burden of Diseases, around 8.3 million cases which is more than half of the 14.3 million global cases and 72000 deaths were recorded in India in 2017 [2]. Currently, there is a worrisome concern with these epidemic instances and the resistance of the bacterium to multiple antibiotics. Early use of the necessary antibiotic medication guards against serious typhoid fever comorbidities. The initial pharmacological therapy of choice is determined by the strains' susceptibility. Fluoroquinolones are the most effective medication of choice in the majority of cases which can be administered empirically based on clinical suspicion in severe circumstances that require immediate treatment before the outcome of the diagnostic culture test. Ciprofloxacin and Ofloxacin are the most efficient fluoroquinolones. Treatment of typhoid with cephalosporins, macrolides, and carbapenems is also extremely successful [3]. For adults, the typical dosage for typhoid fever is 500 mg taken orally every 12 hours for 10 days and for children, the recommended dosage is 500 to 750 mg taken orally every 12 hours for 7-14 days [4, 29]. In endemic locations, strains that are both multidrug-resistant (MDR) and exceptionally drug-resistant (XDR) have emerged. Bacteria are protected from antibiotics by their intracellular nature [5]. More than 1 in 100 people experience the adverse effects of ciprofloxacin. These include nausea, diarrhoea and redness or discomfort in the eye. Serious side effects from ciprofloxacin are extremely rare. Less than one in 100 persons can experience these severe side effects. The serious side effects include muscle weakness, pain or swelling in joints or tendons, severe tiredness, feeling anxious, difficulty sleeping or remembering things, ringing in your ears (tinnitus), loss of taste and smell, irregular heartbeat and sudden breathlessness [6]. As a consequence, there is an urgent need for the establishment of naturally sourced anti-typhoid drugs to manage this situation.

Medicinal plants continue to be a viable source of novel compounds for the creation of pharmaceuticals. *Jatropha curcas* is quickly becoming a highly valuable commercial resource in the creation of novel lead compounds and phytomedicines. The plant is of the family Euphorbiaceae and has a long history of being used medicinally. It is known locally as a psychic nut and is used in traditional folkloric medicine to treat a variety of illnesses, including gonorrhoea, skin infections, jaundice, and fever [7, 8]. Numerous components of this plant, including the leaves, stem bark, and root, have been found to have antibacterial properties.

Salmonella typhi DNA Gyrase B is a subunit in the receptor of Salmonella, which is a multi-domain protein. One possible mechanism of action for the drug's inhibitory activity is the suppression of DNA gyrase which is necessary for chain elongation during chromosome replication in bacterial cells [9]. Beta-lactamase of *Salmonella typhi* inactivates the beta-lactam antibiotic by disrupting the beta-lactam ring [10]. According to a study, typhoid fever patients had an increased concentration of lactate dehydrogenase than that of healthy individuals [11]. The concentration rises rapidly and continuously during the first week of infection before declining and reverting to normal during the fourth and later weeks. The cell necrosis in intestinal lymphatic tissue, which is particularly observed at the onset of the disease, is what primarily causes the rise in lactate dehydrogenase concentration [12]. When the host is infected with the pathogen, the metabolic environment of the gut lumen is changed in a way that favours the pathogen's development at the expense of the microbiota. L-lactate and molecular oxygen are released from the tissue into the intestinal lumen as a result of modifications in host cell metabolism brought on by inflammation. *Salmonella* colonizes the gut by using lactate as an electron donor and oxygen as the terminal electron acceptor [13]. Hence, this study also considers L-lactate dehydrogenase as a potential target. Retinoids are lipophilic isoprenoids made up of a linear chain with a hydrophilic end group and a cyclic group. Retinol, retinal, retinoic acid, retinyl esters, and other derivatives of these molecules are among these substances. Retinoids are excellent pharmaceuticals for skin diseases too. Retinal dehydrogenase transforms retinal into retinoic

© JournalsPub 2023. All Rights Reserved

acid. Retinal dehydrogenase is reported to be present in *Salmonella* [14] and is selected as one of the targets for this study.

The goal of the current work is to identify a prospective therapeutic candidate, by molecular docking, that can inhibit multiple antibacterial targets including DNA Gyrase B, Beta-lactamase, Lactate dehydrogenase, L-Lactate dehydrogenase and Retinal dehydrogenase from various bioactive secondary metabolites found in *Jatropha curcas.* The inhibitory efficiency of the secondary metabolites towards multiple targets expressed in *Salmonella typhi* could help alleviate the symptoms brought on by enteric fever.

MATERIALS & METHODS

Collection of the Ligand Library

Indian Medicinal Plants, Phytochemistry and Therapeutics 2.0 (IMPPAT 2.0) **(**https://cb.imsc.res.in/imppat/**)**, a manually curated database that has been constructed via digitalization of information from more than 100 books on traditional Indian medicine, 7000+ published research articles and other existing resources were used to select a total of 93 phytochemicals from the leaves of *Jatropha curcas* [15, 16]. The PubChem CID, canonical SMILES and the two-dimensional structures of the same were obtained from the PubChem (https://pubchem.ncbi.nlm.nih.gov/) database [17–20].

Protein Retrieval

The three-dimensional crystal structure of the target proteins namely, DNA Gyrase B (5ZXM), Beta-lactamase (1K38), L-lactate dehydrogenase (4OKN) and Lactate dehydrogenase (2V7P) were downloaded in PDB format from Research Collaboratory for Structural Bioinformatics Protein Data Bank (RCSB PDB) (https://www.rcsb.org/) [21]. The FASTA sequence of retinal dehydrogenase was obtained from the NCBI database. The 3D structure of the same was generated using a homology modelling server, SWISS-MODEL (https://swissmodel.expasy.org/). The missing residues were modelled using DS BIOVIA Discovery Studio [22].

Protein Purification

With the aid of DS BIOVIA Discovery Studio, the protein was prepped for docking analysis. Polar hydrogen was added to the receptor during preparation, and the water molecule was removed from the crystallized 3D structure of the receptor before being saved as a PDB file using Discovery Studio software.

Using PDBsum Generate (http://www.ebi.ac.uk/thornton-srv/databases/pdbsum/Generate.html), the purified protein files were utilized to determine each protein's secondary structure and Ramachandran plot. The hydrophobicity plot was generated using DS BIOVIA Discovery Studio.

Molecular Docking

The docking of the ligands to the active site of the target proteins was achieved with the aid of PyRx, a virtual screening tool [23]. The purified proteins in PDB were uploaded to PyRx which are then converted into a macromolecule by adding Kollman charges and assigning every atom as AD4 (AutoDock 4) Type, thereby converting each protein to. pdbqt format. 93 ligands were uploaded in SDF format. Energy minimization was accomplished through the application of a universal force field, therefore converting the ligands to. pdbqt format. The gird dimensions generated for each protein were as follows, DNA Gyrase B (Center X: -11.824 Y: -10.883 Z: 33.6550; and Dimensions (Angstrom) X: 59.7092 Y: 54.6844 Z: 76.2772), Beta-lactamase (Center X: 12.5934 Y: 10.7255 Z: 97.3046; and Dimensions (Angstrom) X: 75.8197 Y: 74.4661 Z: 68.5240), L-Lactate dehydrogenase (Center X: 27.2337 Y: -10.044 Z: -19.3286; and Dimensions (Angstrom) X: 67.3215 Y: 75.9334 Z: 51.4044), Lactate dehydrogenase (Center X: -19.420 Y: 49.8091 Z: 21.9265; and Dimensions (Angstrom) X: 58.0164 Y: 44.6788 Z: 46.3173) and Retinal Dehydrogenase (Center X: 7.5542 Y:

© JournalsPub 2023. All Rights Reserved

4.3804 Z: 10.5559; and Dimensions (Angstrom) X: 61.3565 Y: 66.4763 Z: 77.4457). The ligand-protein docking was achieved and the resulting docking interactions were assessed based on the binding affinity. To achieve the optimum binding conformation with the protein, the ligands adopt nine distinct configurations in PyRx. The optimal docking conformation was determined to be the one with the lowest binding scores among all of the conformations, which corresponds to a binding affinity of zero RMSD (Root Mean Square Deviation) values. The top four conformations with the lowest binding affinity were chosen as the ideal binding complex for each target protein. The docked complexes were downloaded in PDB format and were visualized using DS BIOVIA Discovery Studio software.

Visualization

The docked complexes downloaded from PyRx were visualized using DS BIOVIA Discovery Studio software. The docking complexes were analysed for the interactions of the ligands with amino acids in the protein's binding pocket. The 2D and 3D structures of the interactions were generated.

RESULTS

Ramachandran Plot Statistics

PDBsum Generate was used to generate the Ramachandran plots of Beta-lactamase, DNA Gyrase B, Lactate dehydrogenase, L-Lactate dehydrogenase and Retinal dehydrogenase as shown in Figure 1(b), Figure 2(b), Figure 3(b), Figure 4(b) and Figure 5(b) respectively.

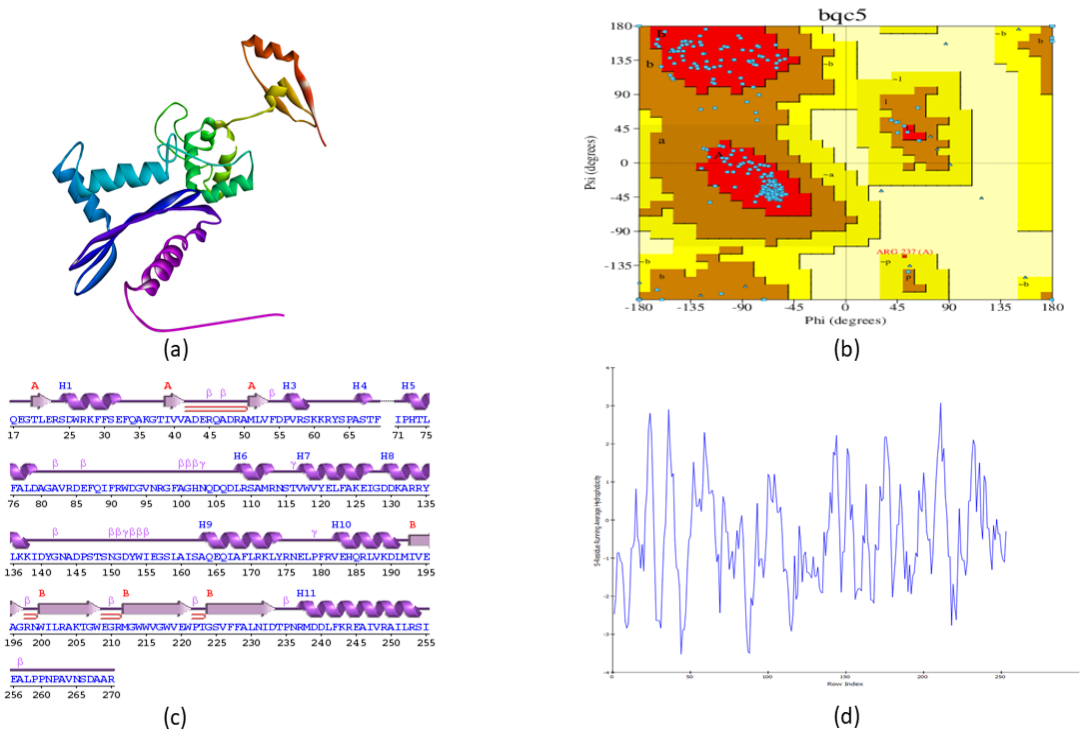

Figure 1. Structural Analysis of Beta-lactamase protein; (a) Purified Beta-lactamase protein structure, (b) Ramachandran plot, (c) Secondary protein structure and (d) Hydrophobicity plot.

- ***Beta-lactamase:*** The purified structure of Beta-lactamase has 83.0% of its residues in the most favoured regions, 16.6% in additionally allowed regions, 0.4% in generously allowed regions and 0.0% in disallowed regions of the Ramachandran plot (Figure 1a).
- ***DNA Gyrase B:*** The Ramachandran plot statistics of the purified structure DNA Gyrase B showed that 91.8% of the residues are in the most favoured regions, 7.6% in additionally allowed regions, 0.0% in generously allowed regions and 0.6% in disallowed regions (Figure 2a).

© JournalsPub 2023. All Rights Reserved

- ***Lactate dehydrogenase:*** 91.6% of the residues of the purified structure of Lactate dehydrogenase are in the most favoured regions, 8.0% in additionally allowed regions, 0.4% in generously allowed regions and 0.0% in disallowed regions of the plot (Figure 3a).

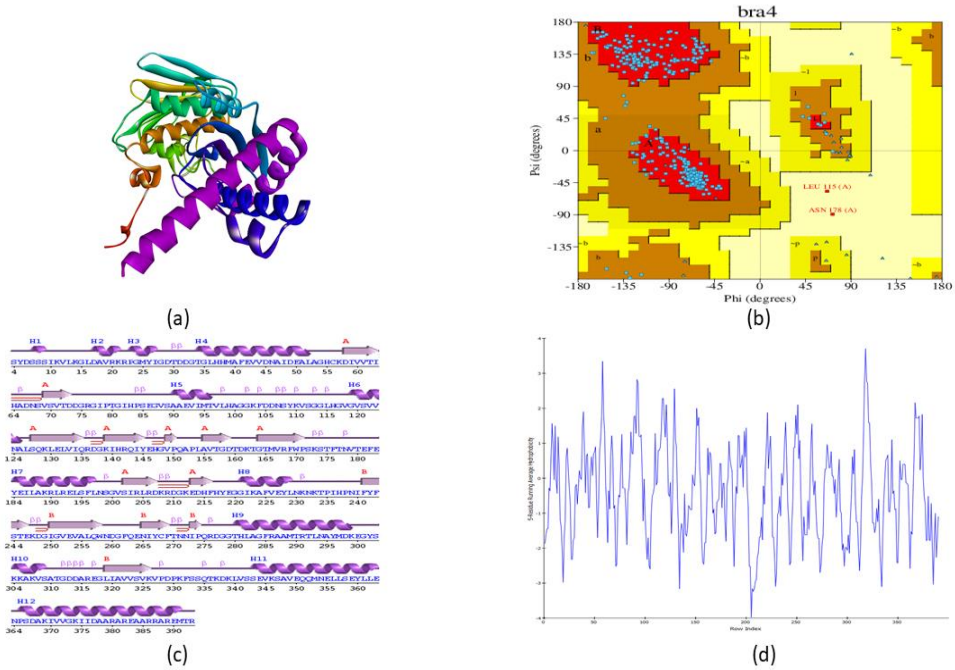

Figure 2. Structural Analysis of DNA Gyrase B protein; (a) Purified DNA Gyrase B protein structure, (b) Ramachandran plot, (c) Secondary protein structure and (d) Hydrophobicity plot.

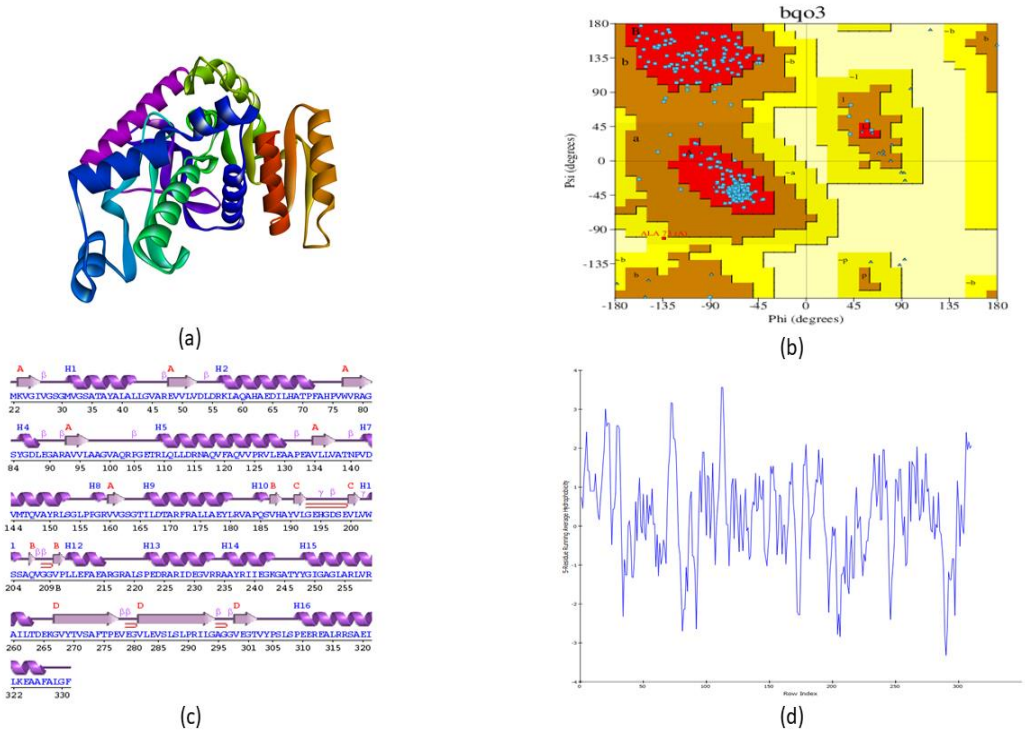

Figure 3. Structural Analysis of Lactate dehydrogenase protein; (a) Purified Lactate dehydrogenase protein structure, (b) Ramachandran plot, (c) Secondary protein structure and (d) Hydrophobicity plot.

© JournalsPub 2023. All Rights Reserved

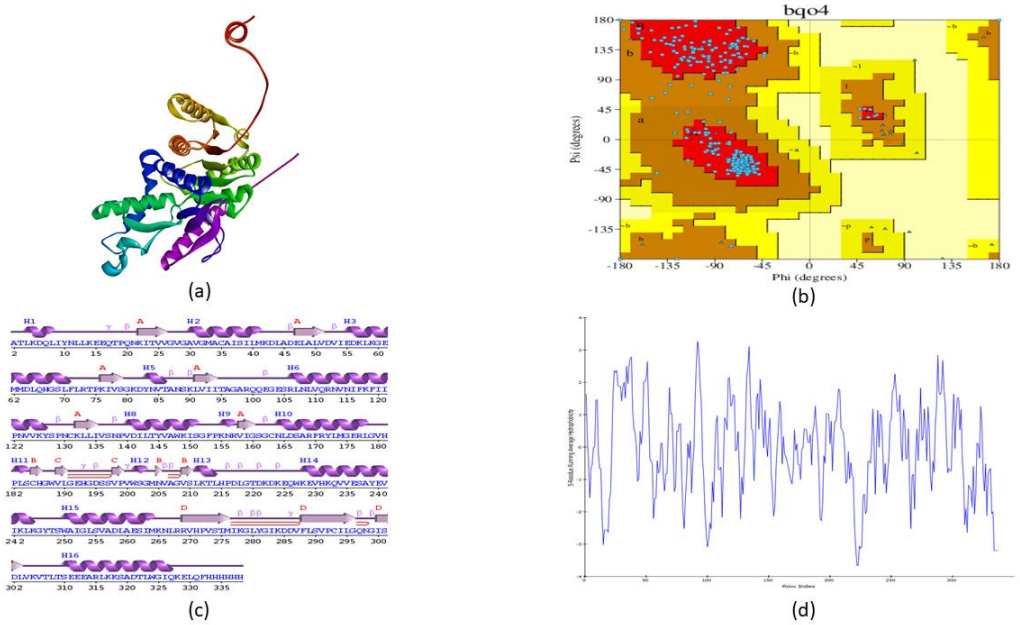

Figure 4. Structural Analysis of L-Lactate dehydrogenase protein; (a) Purified L-Lactate dehydrogenase protein structure, (b) Ramachandran plot, (c) Secondary protein structure and (d) Hydrophobicity plot.

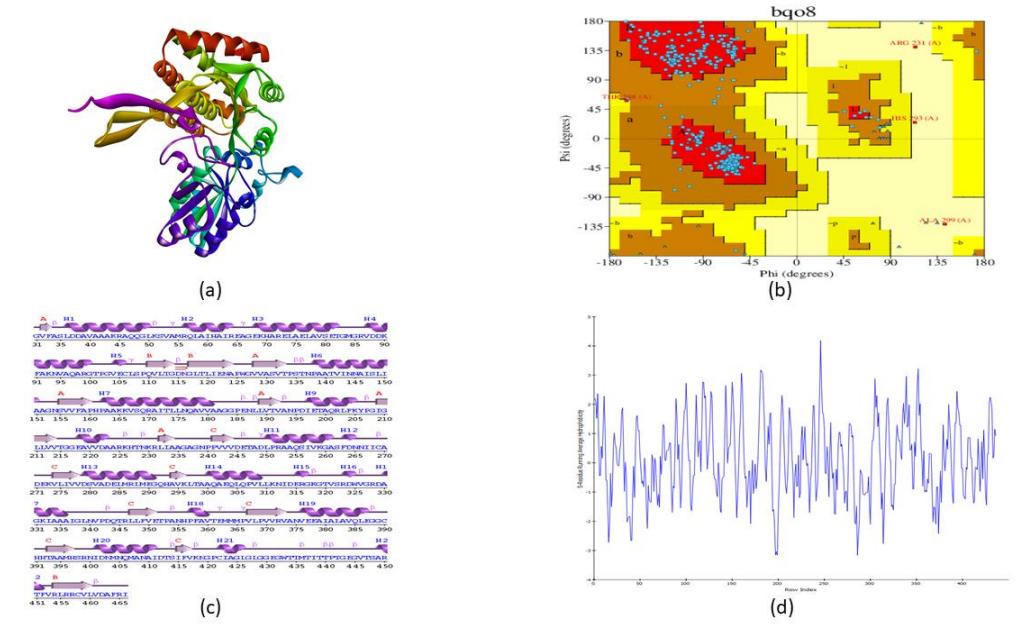

Figure 5. Structural Analysis of Retinal dehydrogenase protein; (a) Purified Retinal dehydrogenase protein structure, (b) Ramachandran plot, (c) Secondary protein structure and (d) Hydrophobicity plot.

- ***L-Lactate dehydrogenase:*** Similarly, the purified structure of L-Lactate dehydrogenase has 89.9% of its residues in the most favoured regions, 10.1% in additionally allowed regions and 0.0% in both generously allowed regions and disallowed regions respectively (Figure 4a).
- ***Retinal dehydrogenase:*** According to the Ramachandran plot statistics of the purified structure of Retinal dehydrogenase, 91.3% of its residues are in the most favoured regions, 7.7% in additionally allowed regions, 0.3% in generously allowed regions and 0.8% in disallowed regions (Figure 5a).

© JournalsPub 2023. All Rights Reserved

Secondary Structure

PDBsum Generate was used to examine the secondary structure of the five proteins namely, Beta-lactamase, DNA Gyrase B, Lactate dehydrogenase, L-Lactate dehydrogenase and Retinal dehydrogenase as depicted in Figure 1(c), Figure 2(c), Figure 3(c), Figure 4(c) and Figure 5(c) respectively.

- ***Beta-lactamase:*** The protein Beta-lactamase's predicted secondary structure includes 2 sheets, 4 beta hairpins, 1 psi loop, 1 beta bulge, 7 strands, 12 helices, 7 helix-helix interacs, 19 beta turns and 4 gamma turns. The structure contains 253 residues in total.
- ***DNA Gyrase B:*** The PDBsum results for this protein's secondary structure prediction are 2 sheets, 6 beta hairpins, 2 psi loops, 4 beta bulges, 14 strands, 12 helices, 13 helix-helix interacs, 37 beta turns and 2 gamma turns. The structure comprises 390 residues in total.
- ***Lactate dehydrogenase:*** In the case of Lactate dehydrogenase, the depicted PDBsum results are 4 sheets, 4 beta alpha beta units, 4 beta hairpins, 3 beta bulges, 14 strands, 16 helices, 22 helix-helix interacs, 15 beta turns and 2 gamma turns. The structure constitutes 310 residues in total.
- ***L-Lactate dehydrogenase:*** For L-Lactate dehydrogenase, PDBsum data shows 4 sheets, 4 beta alpha beta units, 4 beta hairpins, 2 beta bulges, 14 strands, 16 helices, 17 helix-helix interacs, 21 beta turns and 4 gamma turns. The structure comprises 337 residues in total.
- ***Retinal dehydrogenase:*** Finally, the PDBsum outputs for retinal dehydrogenase are 3 sheets, 7 beta alpha beta units, 1 beta hairpin, 1 beta bulge, 16 strands, 22 helices, 19 helix-helix interacs, 26 beta turns and 7 gamma turns. The structure contains 436 residues in total.

Hydrophobicity Plot

The hydrophobicity plots Beta-lactamase, DNA Gyrase B, Lactate dehydrogenase, L-Lactate dehydrogenase and Retinal dehydrogenase were generated and examined using the DS BIOVIA Discovery Studio software, as shown in Figure 1(d), Figure 2(d), Figure 3(d), Figure 4(d) and Figure 5(d) respectively.

Molecular Docking

In this study, a total of 93 ligands were docked against five target proteins of *Salmonella typhi:* Beta-lactamase, DNA Gyrase B, Lactate dehydrogenase, L-Lactate dehydrogenase and Retinal dehydrogenase using PyRx. After docking was completed, the conformation with the lowest binding affinity and zero RMSD value was chosen as the ideal binding complex for each target protein.

The top four ligands with the lowest binding affinity were selected or each protein namely, Beta-lactamase (Table 1), DNA Gyrase B (Table 2), Lactate dehydrogenase (Table 3), L-Lactate dehydrogenase (Table 4) and Retinal dehydrogenase (Table 5).

Table 1. Binding affinity of the top four ligands with Beta-lactamase.

Ligand	Binding affinity
4-(P-Methoxyphenyl)-2-(4-phenyl-2-pyridyl)-6-(2-pyridyl)-pyridine	-11.9
alpha-Amyrin	-9.7
Isovitexin	-9.1
2-Quinazolinamine, 3,4-dihydro-N,3-diphenyl-4-(phenylimino)-	-9.1

Table 2. Binding affinity of the top four ligands with DNA Gyrase B.

Ligand	Binding affinity
4-(P-Methoxyphenyl)-2-(4-phenyl-2-pyridyl)-6-(2-pyridyl)-pyridine	-10.2
2-Quinazolinamine, 3,4-dihydro-N,3-diphenyl-4-(phenylimino)-	-9.4
alpha-Amyrin	-9.2
Isovitexin	-9.1

Table 3. Binding affinity of the top four ligands with Lactate dehydrogenase.

Ligand	Binding affinity
Isovitexin	-9.5
4-(P-Methoxyphenyl)-2-(4-phenyl-2-pyridyl)-6-(2-pyridyl)-pyridine	-8.9
Apigenin	-8.3
Vitexin	-8.1

© JournalsPub 2023. All Rights Reserved

Table 4. Binding affinity of the top four ligands with L-Lactate dehydrogenase.

Ligand	Binding affinity
4-(P-Methoxyphenyl)-2-(4-phenyl-2-pyridyl)-6-(2-pyridyl)-pyridine	-9.3
alpha-Amyrin	-8.9
beta-Sitosterol-beta-D-glucoside	-8.8
2-Quinazolinamine, 3,4-dihydro-N,3-diphenyl-4-(phenylimino)-	-8.7

Table 5. Binding affinity of the top four ligands with Retinal dehydrogenase.

Ligand	Binding affinity
4-(P-Methoxyphenyl)-2-(4-phenyl-2-pyridyl)-6-(2-pyridyl)-pyridine	-8.7
Isovitexin	-7.9
2-Quinazolinamine, 3,4-dihydro-N,3-diphenyl-4-(phenylimino)-	-7.9
Campesterol	-7.0

Comparison with Binding Affinities of WHO Approved Drugs:

The 2D structures of Ciprofloxacin and Ofloxacin were downloaded from PubChem and docked against the five target proteins using PyRx. After completion, the binding affinity values of Ciprofloxacin was found to be -7.6 with the protein Beta-lactamase, -7.5 with DNA Gyrase B, -7.0 with Lactate dehydrogenase, -6.7 with L-Lactate dehydrogenase and -6.4 with Retinal dehydrogenase. Similarly, the binding affinity of Ofloxacin was -8.1 with Beta-lactamase, -7.2 with DNA Gyrase B, -7.8 with Lactate dehydrogenase, -8.2 with L-Lactate dehydrogenase and -6.5 with Retinal dehydrogenase.

The phytocompounds obtained from *Jatropha curcas* had better binding affinity values with the target proteins when compared to Ciprofloxacin and Ofloxacin. Hence, this could be used as a potential approach to tackle drug resistance.

Visualization

The selected ligands were then visualized using DS BIOVIA Discovery Studio software. The 3D and 2D models of the same were generated. Moreover, the interactions of the ligands with amino acids in the protein's binding pocket were analysed. The forces involved in protein-ligand interaction of this study are hydrogen bonding, hydrophobic and electrostatic interactions (Figures 6-10)

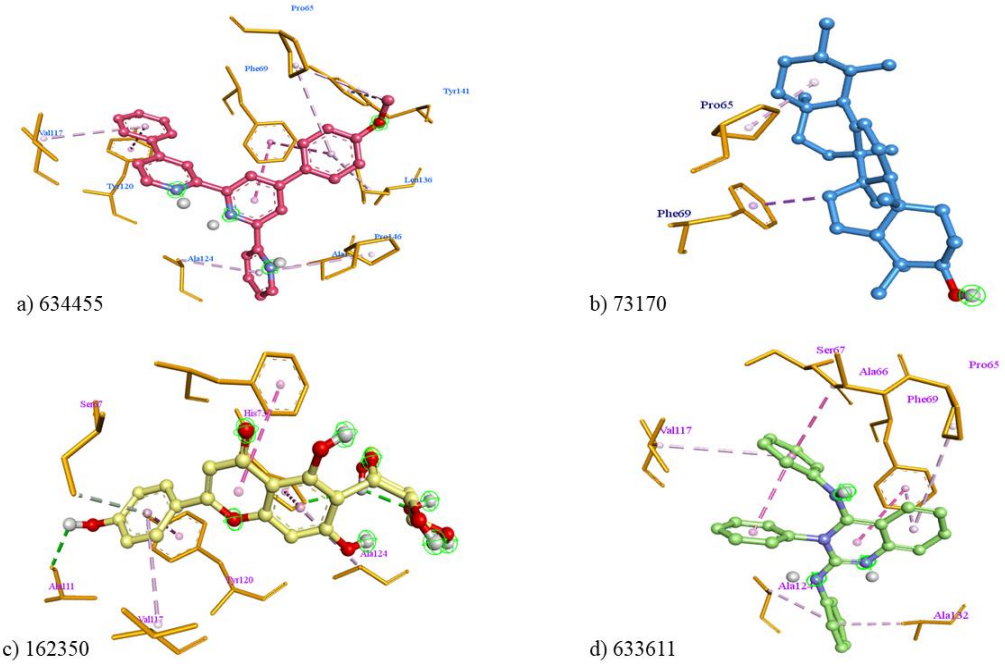

Figure 6. Interactions of top ligands with Beta-lactamase.

© JournalsPub 2023. All Rights Reserved

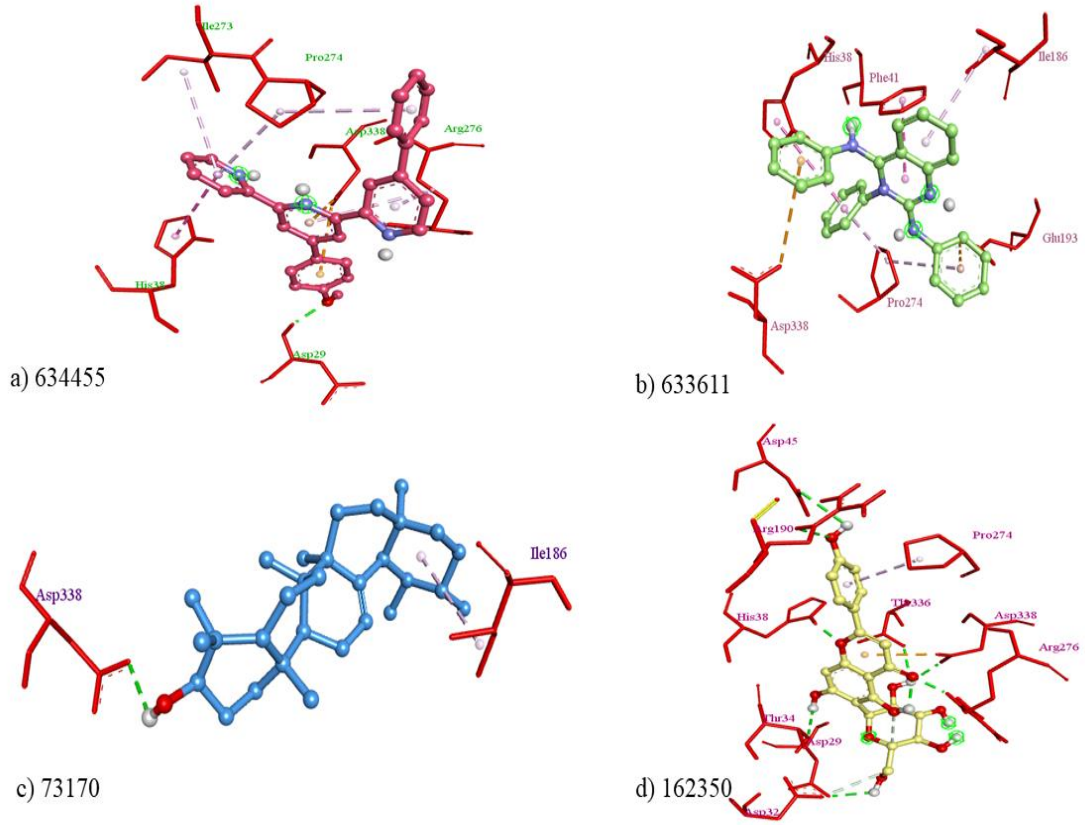

Figure 7. Interactions of top ligands with DNA Gyrase B.

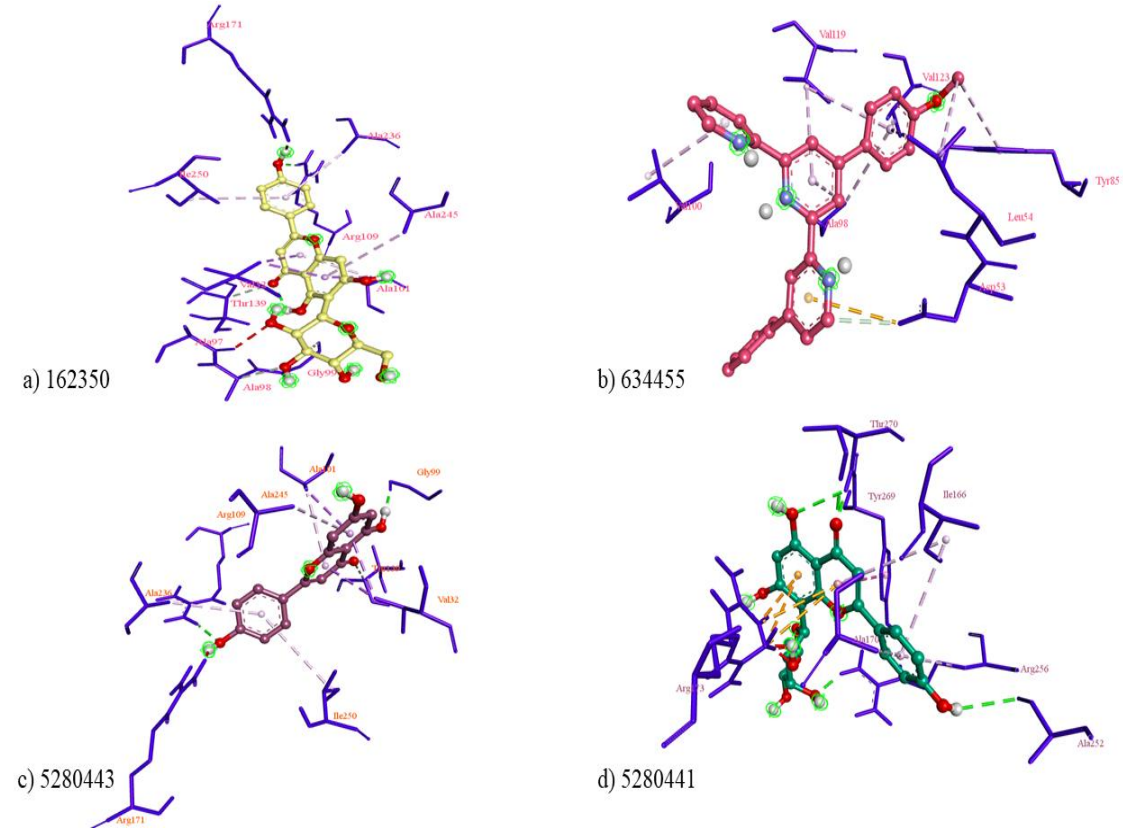

Figure 8. Interactions of top ligands with Lactate dehydrogenase.

© JournalsPub 2023. All Rights Reserved

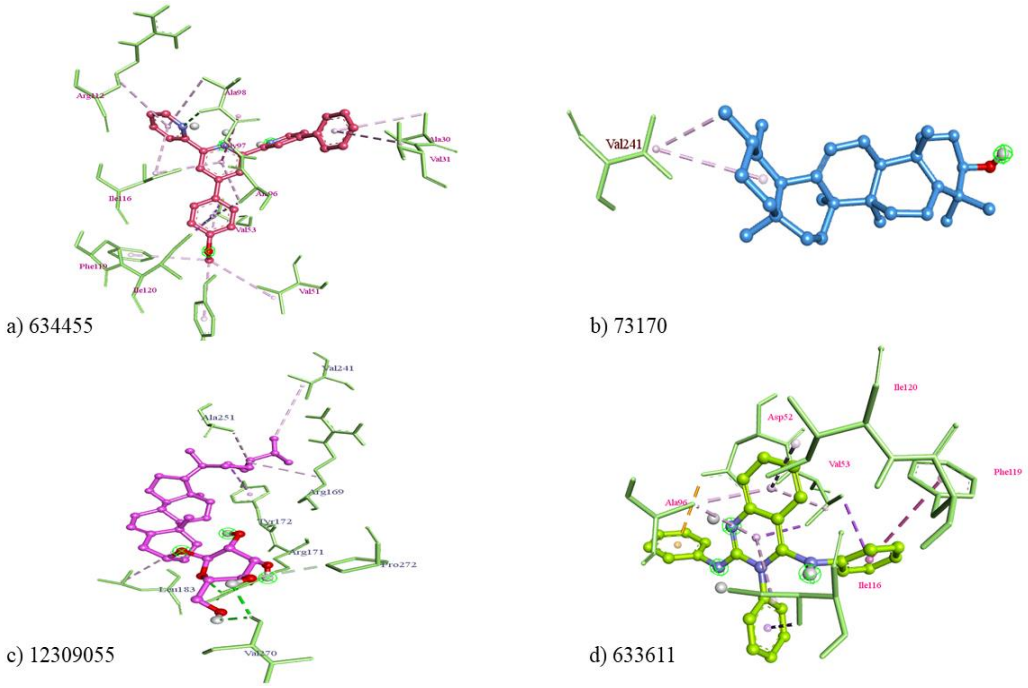

Figure 9. Interactions of top ligands with L-Lactate dehydrogenase.

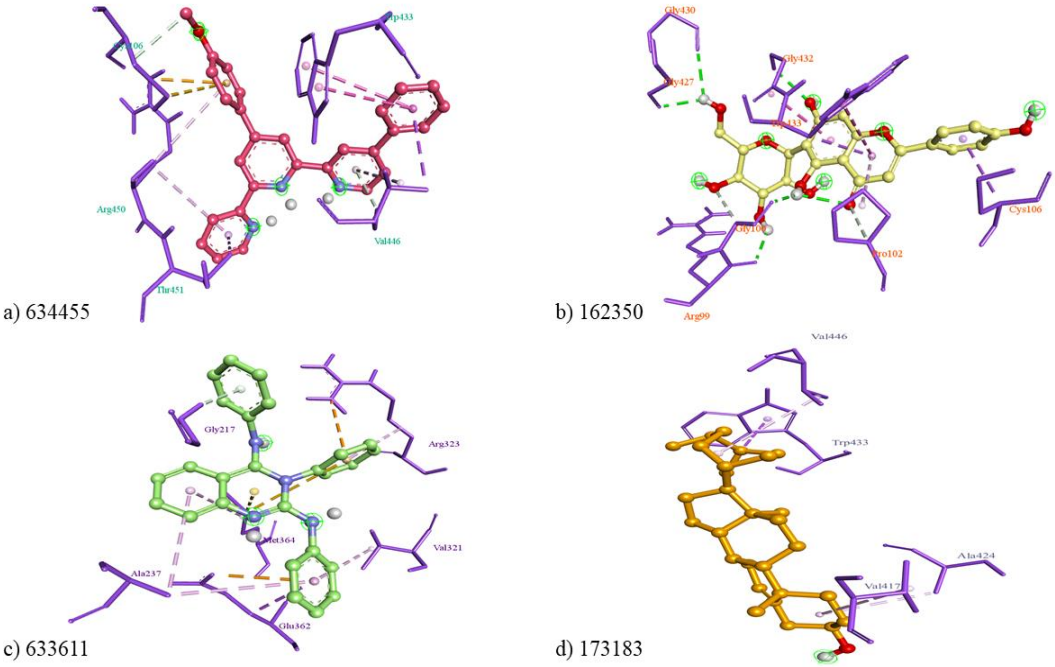

Figure 10. Interactions of top ligands with Retinal dehydrogenase.

ADMET Analysis

With the aid of ADMET Lab 2.0, 14 ligands namely alpha-Amyrin (PubChem CID: 73170), 4-(P-Methoxyphenyl)-2-(4-phenyl-2-pyridyl)-6-(2-pyridyl)-pyridine (PubChem CID: 634455), 2-Quinazolinamine, 3,4-dihydro-N,3-diphenyl-4-(phenylimino)- (PubChem CID: 633611), Campesterol (PubChem CID: 173183), beta-Sitosterol (PubChem CID: 222284), Isovitexin (PubChem CID: 162350), beta-Sitosterol-beta-D-glucoside (PubChem CID: 12309055), Vitexin (PubChem CID: 5280441), Apigenin (PubChem CID: 5280443), Stigmasterol (PubChem CID: 5280794), N-hydroxy-N'-[2-(trifluoromethyl)phenyl]pyridine-3-carboximidamide (PubChem CID: 550559), Lanosta-

© JournalsPub 2023. All Rights Reserved

7,9(11)-diene-3,18,20-triol (PubChem CID: 91695604), 4-Pregnene-3,6,20-trione-tri-methyl oxime (PubChem CID: 91745029) and 1,7-Dicyclohexyl-4-(3-cyclohexylpropyl)heptane (PubChem CID: 296571) were examined for their physiochemical properties, medicinal chemistry, absorption, distribution, and toxicity as depicted in the tables 6-11 below.

Table 6. Physiochemical Properties of the top derivatives of Jatropha curcas.

PubChem ID	MW	Vol	nHA	nHD	nRot	nRing	nHet	fChar	Flex	TPSA	LogS
73710	426.39	426.39	1	1	0	5	1	0	0	20.23	-6.357
634455	415.17	415.17	4	0	5	5	4	0	0.167	47.9	-6.927
633611	388.17	388.17	4	1	3	5	4	0	0.097	45.44	-6.198
173183	400.37	400.37	1	1	5	4	1	0	0.25	20.23	-7.006
222284	414.39	414.39	1	1	6	4	1	0	0.3	20.23	-7.052
162350	432.11	432.11	10	7	3	4	10	0	0.125	181.05	-3.754
12309055	576.44	576.44	6	4	9	5	6	0	0.346	99.38	-4.432
5280441	432.11	432.11	10	7	3	4	10	0	0.125	181.05	-3.779
5280443	270.05	270.05	5	3	1	3	5	0	0.056	90.9	-3.606
5280794	412.37	412.37	1	1	5	4	1	0	0.238	20.23	-6.978
550559	281.08	281.08	4	2	4	2	7	0	0.308	57.51	-3.256
91695604	458.38	458.38	3	3	6	4	3	0	0.3	60.69	-4.723
91745029	415.28	415.28	6	0	4	4	6	0	0.174	64.77	-5.923
296571	388.41	388.41	0	0	12	3	0	0	0.667	0	-7.775

MW: Molecular weight; Vol: Volume; nHA: Number of hydrogen bond acceptors; nHD: Number of hydrogen bond donors; nRot: Number of rotatable bonds; nRing: Number of rings; nHet: Number of heteroatoms; fChar: Formal charge; Flex: Flexibility; TPSA: Topological Polar Surface Area; LogS: Log of the aqueous solubility.

Table 7. Medicinal Properties of the top derivatives of Jatropha curcas.

PubChem ID	QED	PAINS	Lipinski	Fsp3	SA Score
73710	0.389	0	Accepted	0.933	4.695
634455	0.327	0	Accepted	0.036	2.172
633611	0.429	0	Accepted	0	2.593
173183	0.47	0	Accepted	0.929	4.35
222284	0.436	0	Accepted	0.931	4.388
162350	0.3	0	Accepted	0.286	3.943
12309055	0.257	0	Rejected	0.943	4.99
5280441	0.3	0	Accepted	0.286	3.954
5280443	0.632	0	Accepted	0	2.253
5280794	0.457	0	Accepted	0.862	4.571
550559	0.384	0	Accepted	0.077	2.389
91695604	0.43	0	Accepted	0.867	5.011
91745029	0.468	0	Accepted	0.792	4.841
296571	0.312	0	Accepted	1	2.144

QED: Quantitative estimate of drug-likeness; PAINS: Pan Assay Interference Compounds; Fsp3: Number of sp3 hybridized carbons / total carbon count; SA Score: Synthetic Accessibility Score.

Table 8. Absorption Properties of the top derivatives of Jatropha curcas.

PubChem ID	Caco-2	MDCK	Pgp-inh	Pgp-sub	HIA	F(20%)
73710	-4.953	6.85E-06	0.181	0	0.008	0.434
634455	-4.721	1.16E-05	0.962	0.973	0.003	0.859
633611	-4.931	2.72E-05	0.022	0.028	0.053	0.999
173183	-4.74	8.91E-06	0.377	0.001	0.004	0.013
222284	-4.756	8.63E-06	0.341	0.001	0.004	0.01
162350	-5.939	1.57E-05	0.001	0.767	0.876	0.965
12309055	-4.785	2.05E-05	0.248	0.004	0.018	0.015
5280441	-6.082	1.61E-05	0.001	0.795	0.884	0.919
5280443	-4.847	1.16E-05	0.004	0.82	0.015	0.995
5280794	-4.668	7.52E-06	0.066	0.001	0.005	0.008
550559	-4.382	2.47E-05	0.003	0.011	0.005	0.001
91695604	-4.76	1.19E-05	0.971	0	0.014	0.037
91745029	-5.031	1.46E-05	0.998	0.001	0.051	0.755
296571	-4.97	7.16E-06	0	0.009	0.002	0.044

Caco-2: Caco-2 permeability; MDCK: MDCK (Madin-Darby canine kidney) permeability; Pgp-inh: Pgp-inhibitor; Pgp-sub: Pgp-substrate; HIA: Human Intestinal Absorption; F(20%): 20% Bioavailability.

© JournalsPub 2023. All Rights Reserved

Table 9. Distribution Properties of the top derivatives of Jatropha curcas.

PubChem ID	BBB	PPB	VDss	Fu
73710	0.762	99.70%	1.831	1.81%
634455	0.336	100.17%	1.737	0.74%
633611	0.483	97.99%	1.958	1.16%
173183	0.854	98.68%	1.842	1.79%
222284	0.84	98.31%	1.963	1.48%
162350	0.04	90.31%	0.983	11.71%
12309055	0.059	97.24%	1.44	1.81%
5280441	0.033	88.82%	1.026	12.07%
5280443	0.012	97.25%	0.51	3.67%
5280794	0.691	98.67%	2.408	1.57%
550559	0.427	83.96%	3.424	17.43%
91695604	0.356	97.19%	1.211	1.98%
91745029	0.935	81.69%	2.757	7.68%
296571	0.001	98.38%	4.238	0.27%

BBB: Blood-Brain Barrier Penetration; PPB: Plasma Protein Binding; VDss: Volume Distribution; Fu: Fraction unbound in plasms.

Table 10. Metabolism and Excretion Properties of the top derivatives of Jatropha curcas.

PubChem ID	CYP1A2-inh	CYP1A2-sub	CYP3A4-inh	CYP3A4-sub	CL	T1/2
73710	0.026	0.454	0.217	0.745	17.973	0.008
634455	0.854	0.179	0.171	0.162	3.958	0.035
633611	0.961	0.72	0.718	0.676	2.546	0.204
173183	0.055	0.523	0.181	0.769	17.948	0.015
222284	0.044	0.491	0.202	0.784	16.686	0.013
162350	0.043	0.042	0.021	0.022	1.97	0.481
12309055	0.002	0.346	0.085	0.46	5.939	0.016
5280441	0.05	0.042	0.037	0.024	3.397	0.534
5280443	0.988	0.145	0.833	0.126	7.022	0.856
5280794	0.041	0.603	0.339	0.852	15.958	0.014
550559	0.786	0.44	0.718	0.233	0.908	0.492
91695604	0.014	0.145	0.562	0.663	13.159	0.033
91745029	0.018	0.762	0.565	0.871	0.251	0.038
296571	0.028	0.148	0.159	0.046	4.864	0.004

CL: Clearance; T1/2: Half-life.

Table 11. Toxicity Properties of the top derivatives of Jatropha curcas.

PubChem ID	hERG	H-HT	DILI	Ames	Carcinogenicity	Respiratory Toxicity	IGC50	LC50
73710	0.003	0.133	0.012	0.011	0.017	0.967	5.455	6.821
634455	0.378	0.574	0.925	0.663	0.338	0.266	5.358	7.254
633611	0.183	0.975	0.955	0.904	0.786	0.237	5.178	6.053
173183	0.04	0.193	0.281	0.032	0.067	0.502	4.855	4.972
222284	0.049	0.16	0.203	0.026	0.047	0.536	4.984	5.365
162350	0.07	0.118	0.954	0.709	0.052	0.041	4.145	4.751
12309055	0.04	0.177	0.085	0.068	0.038	0.72	4.917	5.307
5280441	0.021	0.154	0.975	0.795	0.06	0.041	4.055	4.965
5280443	0.057	0.072	0.854	0.475	0.277	0.266	4.588	5.208
5280794	0.012	0.011	0.055	0.029	0.054	0.19	4.978	5.511
550559	0.027	0.464	0.974	0.028	0.123	0.97	3.257	4.144
91695604	0.082	0.652	0.002	0.015	0.086	0.961	4.723	5.306
91745029	0.424	0.336	0.542	0.019	0.052	0.936	4.829	6.161
296571	0.841	0.072	0.506	0.011	0.019	0.042	6.12	3.883

hERG: The human Ether-à-go-go-Related Gene; H-HT: Human Hepatotoxicity; DILI: Drug Induced Liver Injury; Ames: The Ames Toxicity Test.

DISCUSSION

Typhoid is a potentially fatal bacterial infection that is spread by consuming unsanitary food or drink that has been contaminated with faeces. Since filthy conditions are more likely to exist in low-income countries, this infection is more frequently seen there. But the disease still poses a threat to

© JournalsPub 2023. All Rights Reserved

public health in underdeveloped countries of Africa, the Americas, South-East Asia, and the Western Pacific. According to the WHO, there are 9 million cases of typhoid fever worldwide each year, and between 110 000 people die from the disease [28].

Since there are no animal reservoirs for *Salmonella typhi*, the most prevalent method of transmission is through the faecal-oral route, in which food and drink are contaminated with human faeces. After an incubation period of a week or two, typhoid fever clinical signs begin. Acute typhoid fever is characterized by a protracted step-ladder pattern of fever, gastrointestinal problems, malaise, headache, and anorexia [25]. Some of the patients also have "rose spots" (exanthem) on their back, chest, and belly. Obscured blood in the faeces, intestinal perforation, and peritonitis may be symptoms of the disease's complications, which are then followed by hypotension, bradycardia, abdominal discomfort, and rigidity. These instances are on the rise, and *Salmonella typhi* is becoming increasingly resistant to antibiotics like streptomycin, chloramphenicol, trimethoprim-sulfamethoxazole, ampicillin, and ciprofloxacin, which poses an alarming problem.

Computational methods offer the advantages of being quick and affordable in this context, but what's more significant is that they let researchers ask questions that would be challenging to answer empirically. These *in silico* investigations are frequently employed and have become an essential part of drug development and discovery programs [24].

The treatment of different illnesses, particularly bacterial infections, is greatly aided by medicinal herbs like *Jatropha curcas*. Previous research has shown that the phytocompounds of this plant have effective antimicrobial effects [25] and also enhance the bioactivity of medicinal plants and therefore aid in antibacterial activity too [26].

In this study, the antibacterial effectiveness of 93 phytocompounds against *Salmonella typhi* was assessed. The ligands 4-(P-Methoxyphenyl)-2-(4-phenyl-2-pyridyl)-6-(2-pyridyl)-pyridine, alpha-Amyrin, Isovitexin and 2-Quinazolinamine, 3,4-dihydro-N,3-diphenyl-4-(phenylimino)- had the binding affinities -11.9, -9.7, -9.1 and -9.1 respectively against the protein Beta-lactamase and were further visualized. The same ligands exhibited the lowest binding affinity values against the protein DNA Gyrase B in the decreasing order of 4-(P-Methoxyphenyl)-2-(4-phenyl-2-pyridyl)-6-(2-pyridyl)-pyridine, 2-Quinazolinamine, 3,4-dihydro-N,3-diphenyl-4-(phenylimino)-, alpha-Amyrin and Isovitexin having binding affinity values -10.2, -9.4, -9.2 and -9.1 respectively [28]. Whereas the ligands Isovitexin, 4-(P-Methoxyphenyl)-2-(4-phenyl-2-pyridyl)-6-(2-pyridyl)-pyridine, Apigenin and Vitexin with binding affinities -9.5, -8.9, -8.3 and -8.1 respectively were selected for the protein Lactate dehydrogenase. Similarly, 4-(P-Methoxyphenyl)-2-(4-phenyl-2-pyridyl)-6-(2-pyridyl)-pyridine, alpha-Amyrin, beta-Sitosterol-beta-D-glucoside and 2-Quinazolinamine, 3,4-dihydro-N,3-diphenyl-4-(phenylimino)- having binding affinities -9.3, -8.9, -8.8 and -8.7 respectively were chosen for L-Lactate dehydrogenase. For Retinal dehydrogenase, the ligands 4-(P-Methoxyphenyl)-2-(4-phenyl-2-pyridyl)-6-(2-pyridyl)-pyridine, Isovitexin, 2-Quinazolinamine, 3,4-dihydro-N,3-diphenyl-4-(phenylimino)- and Campesterol were selected based on their binding affinity values -8.7, -7.9, -7.9 and -7.0 respectively. These interactions were visualized using DS BIOVIA Discovery Studio software.

On analysing the 2D structures of the top four ligands docked with the protein Beta-lactamase, the amino acids VAL A: 117, PHE A: 69, ALA A: 124 and PRO A: 65 were found to be common. Whereas, in the case of the top four ligands complexed with DNA Gyrase B, the common amino acids were ASP A: 338 and PRO A: 274. However, the 2D structures of the top four ligands docked with the proteins Lactate dehydrogenase, L-Lactate dehydrogenase and Retinal dehydrogenase exhibited zero amino acids as common.

The ligands were then evaluated for their ADMET properties as it is vital to know the adsorption, distribution, metabolism, excretion and toxicity properties of the drugs. 14 compounds were screened using ADMET Lab 2.0 and were examined for their pharmacokinetic and medicinal properties

© JournalsPub 2023. All Rights Reserved

(Tables 6-11). So, in the current investigation, an effort has been made to develop pharmacological candidates that can suppress bacterial development. The derivatives of different significant phytochemicals from the plant demonstrated some encouraging protein target inhibitory action. The current study thus provides a window into the investigation of potential replacement medications for the current antibiotics.

CONCLUSION

In the present study, various phytocompounds from the plant *Jatropha curcas* were studied and the results obtained demonstrate that it has a strong potential as a therapeutic candidate, particularly against disorders linked to *Salmonella typhi*. Because of their antibacterial capabilities, this study suggests that these plants have great promise for the creation of phytomedicines. According to this study, the ligand 4-(P-Methoxyphenyl)-2-(4-phenyl-2-pyridyl)-6-(2-pyridyl)-pyridine has the best binding affinity for the proteins Beta-lactamase (-11.9), DNA Gyrase B (-10.2), L-lactate dehydrogenase (-9.3) and Retinal dehydrogenase (-8.7) whereas the ligand Isovitexin had the best binding affinity for the protein Lactate dehydrogenase (-9.5). These compounds can be further studied through *in vitro* techniques.

Acknowledgement

I would like to thank Ms Susha Dinesh for her assistance throughout the project, as well as BioNome for offering computational facilities and support in scientific research services.

REFERENCES

1. Moudgil KD, Narang BS, Pathogenesis of typhoid fever. Indian journal of paediatrics. 1985 Jul-Aug; [PubMed PMID: 4093170]
2. Stanaway JD, Reiner RC, Blacker BF, et al.The global burden of typhoid and paratyphoid fevers: a systematic analysis for the Global Burden of Disease Study 2017. Lancet Infect Dis 2019;19:369–81. https://www.sciencedirect.com/science/article/pii/S1473309918306856
3. Typhoid fever - Diagnosis and treatment - Mayo Clinic. Mayoclinic.org. Published 2023. Accessed April 24, 2023. https://www.mayoclinic.org/diseases-conditions/typhoid-fever/diagnosis-treatment/drc-20378665
4. Wen SC, Best E, Nourse C, Non-typhoidal Salmonella infections in children: Review of literature and recommendations for management. Journal of paediatrics and child health. 2017 Oct [PubMed PMID: 28556448]
5. NHS Choices. Side effects of ciprofloxacin - Brand names: Ciproxin, Ciloxan, Cetraxal. Published 2023. Accessed April 24, 2023. https://www.nhs.uk/medicines/ciprofloxacin/side-effects-of-ciprofloxacin/
6. Dalziel JM. The Useful Plants of West Tropical Africa. Crown Agents for the Colonies, London. (1937)
7. Chopra RN, Nayar SL, Chopra JC. Glossary of Indian Medicinal Plants. Council of Scientific and Industrial Research, New Delhi, (1956)
8. Kourlaba, G., Gkrania-Klotsas, E., Kourkouni, E., Mavrogeorgos, G. and Zaoutis, T. E. (2016). Antibiotic prescribing and expenditures in outpatient adults in Greece, 2010 to 2013: evidence from real-world practice. Eurosurveillance, 21:30266.
9. Molecular docking analysis of beta-lactamase from Salmonella species with eicosane V. Nagasinduja1, S. Shahitha1, B. Prakash2 & D. Jegadeesh Kumar3 1Department of Microbiology, Muthayammal College of Arts & Science, Namakkal, Tamil Nadu, India; 2Department of Biotechnology, Vels Institute of Science Technology & Advanced Studies, Chennai, Tamil Nadu, India; 3Chromopark Research Centre, Namakkal, Tamil Nadu, India
10. Evaluation of serum lactate dehydrogenase levels in typhoid fever January 2013, International Journal of Pharma and Bio Sciences 4(1): B944-B950 Authors: Kasun Sameera, Thota Sunitha, P. Naveen Kumar, P. Sujatha
11. Fumagalli G. Comportamento delle latticodeidrogenasi nell'infezione tifoidea [Behavior of lactate dehydrogenase in typhoid infection]. Minerva Med. 1977 Apr 14;68(18):1199-204. Italian. PMID: 870847.

© JournalsPub 2023. All Rights Reserved

12. Gillis CC, Winter MG, Chanin RB, Zhu W, Spiga L, Winter SE. Host-Derived Metabolites Modulate Transcription of *Salmonella* Genes Involved in l-Lactate Utilization during Gut Colonization. Infect Immun. 2019 Mar 25;87(4):e00773-18. doi: 10.1128/IAI.00773-18. PMID: 30617205; PMCID: PMC6434127.
13. Jang, HJ., Yoon, SH., Ryu, HK. et al. Retinoid production using metabolically engineered Escherichia coli with a two-phase culture system. Microb Cell Fact 10, 59 (2011). https://doi.org/10.1186/1475-2859-10-59
14. IMPPAT: A curated database of Indian Medicinal Plants, Phytochemistry, And Therapeutics, Karthikeyan Mohanraj#, Bagavathy Shanmugam Karthikeyan#, R.P. Vivek-Ananth#, R.P. Bharath Chand, S.R. Aparna, P. Mangalapandi and Areejit Samal*, Scientific Reports 8:4329 (2018).
15. IMPPAT 2.0: an enhanced and expanded phytochemical atlas of Indian medicinal plants, R. P. Vivek-Ananth, Karthikeyan Mohanraj, Ajaya Kumar Sahoo and Areejit Samal*, bioRxiv 2022.06.17.496609 (2022).
16. AMA Kim S, Chen J, Cheng T, et al. PubChem in 2021: new data content and improved web interfaces. Nucleic Acids Res. 2021;49(D1):D1388–D1395. doi:10.1093/nar/gkaa971
17. MLA Kim, Sunghwan, et al. "PubChem in 2021: new data content and improved web interfaces." Nucleic Acids Res. vol. 49, D1 (2021): D1388-D1395. doi:10.1093/nar/gkaa971
18. APA Kim, S., Chen, J., Cheng, T., Gindulyte, A., He, J., He, S., Li, Q., Shoemaker, B. A., Thiessen, P. A., Yu, B., Zaslavsky, L., Zhang, J., & Bolton, E. E. (2019). PubChem in 2021: new data content and improved web interfaces. Nucleic Acids Res., 49(D1), D1388–D1395. https://doi.org/10.1093/nar/gkaa971
19. NLM Kim S, Chen J, Cheng T, Gindulyte A, He J, He S, Li Q, Shoemaker BA, Thiessen PA, Yu B, Zaslavsky L, Zhang J, Bolton EE. PubChem in 2021: new data content and improved web interfaces. Nucleic Acids Res. 2019 Jan 8;47(D1): D1388-D1395. doi: 10.1093/nar/gkaa971. PMID: 33151290.
20. H.M. Berman, J. Westbrook, Z. Feng, G. Gilliland, T.N. Bhat, H. Weissig, I.N. Shindyalov, P.E. Bourne. (2000) The Protein Data Bank Nucleic Acids Research, 28: 235-242.
21. BIOVIA, Dassault Systèmes, BIOVIA DISCOVERY STUDIO, v21.1.0.20298, San Diego: Dassault Systèmes, 2021.
22. Small-Molecule Library Screening by Docking with PyRx. Dallakyan S, Olson AJ. Methods Mol Biol. 2015;1263:243-50
23. Akinyemi, K.O., Smith, S. I., Oyefolu, A. O. and Coker, A. O. Multidrug resistance in Salmonella enterica serovar typhi isolated from patients with typhoid fever complications in Lagos, Nigeria. Public Health, 2005; 119:321-327.
24. Bajorath J. Nat Rev Drug Discov, 2002; 1:882–894
25. Cowan MM. Plant products as antimicrobial agents. Clin. Microbiol. 1999;12:564-582.
26. Motar MLR, Thomas G, Barbosa Fillo JM. Effects of Anarcadium occidentale stem bark extract on in vivo inflammatory models. J. Ethnopharm. 1985;95:139-142.
27. https://www.facebook.com/Drugscom. Ciprofloxacin Dosage Guide + Max Dose, Adjustments [Internet]. Drugs.com. Drugs.com; 2022. Available from: https://www.drugs.com/dosage/ciprofloxacin.html#Usual_Adult_Dose_for_Typhoid_Fever
28. Typhoid [Internet]. Who.int. 2023. Available from: https://www.who.int/teams/immunization-vaccines-and-biologicals/diseases/typhoid

© JournalsPub 2023. All Rights Reserved